Integrated liquid-core optical fibers for ultra-efficient nonlinear liquid photonics

K. Kieu,* L. Schneebeli, R. A. Norwood, and N. Peyghambarian

College of Optical Sciences, University of Arizona, Tucson, Arizona 85721, USA
**kkieu@optics.arizona.edu*

Abstract: We have developed a novel integrated platform for liquid photonics based on liquid core optical fiber (LCOF). The platform is created by fusion splicing liquid core optical fiber to standard single-mode optical fiber making it fully integrated and practical - a major challenge that has greatly hindered progress in liquid-photonic applications. As an example, we report here the realization of ultralow threshold Raman generation using an integrated CS_2 filled LCOF pumped with sub-nanosecond pulses at 532nm and 1064nm. The measured energy threshold for the Stokes generation is 1nJ, about three orders of magnitude lower than previously reported values in the literature for hydrogen gas, a popular Raman medium. The integrated LCOF platform opens up new possibilities for ultralow power nonlinear optics such as efficient white light generation for displays, mid-IR generation, slow light generation, parametric amplification, all-optical switching and wavelength conversion using liquids that have orders of magnitude larger optical nonlinearities compared with silica glass.

OCIS codes: (060.4370) Nonlinear optics, fibers; (160.4330) Nonlinear optical materials.

References and links

1. D. Psaltis, S. R. Quake, and C. Yang, "Developing optofluidic technology through the fusion of microfluidics and optics," Nature **442**(7101), 381–386 (2006).
2. C. Monat, P. Domachuk, and B. J. Eggleton, "Integrated optofluidics: a new river of light," Nat. Photonics **1**(2), 106–114 (2007).
3. E. P. Ippen, "Low-power quasi-CW Raman oscillator," Appl. Phys. Lett. **16**(8), 303–305 (1970).
4. J. Stone, "CW Raman fiber amplifier," Appl. Phys. Lett. **26**(4), 163–165 (1975).
5. F. Benabid, J. C. Knight, G. Antonopoulos, and P. S. J. Russell, "Stimulated Raman scattering in hydrogen-filled hollow-core photonic crystal fiber," Science **298**(5592), 399–402 (2002).
6. T. T. Larsen, A. Bjarklev, D. S. Hermann, and J. Broeng, "Optical devices based on liquid crystal photonic bandgap fibres," Opt. Express **11**(20), 2589–2596 (2003).
7. F. Benabid, F. Couny, J. C. Knight, T. A. Birks, and P. S. J. Russell, "Compact, stable and efficient all-fibre gas cells using hollow-core photonic crystal fibres," Nature **434**(7032), 488–491 (2005).
8. J. Bethge, A. Husakou, F. Mitschke, F. Noack, U. Griebner, G. Steinmeyer, and J. Herrmann, "Two-octave supercontinuum generation in a water-filled photonic crystal fiber," Opt. Express **18**, 62306240 (2010).
9. M. C. P. Huy, A. Baron, S. Lebrun, R. Frey, and P. Delaye, "Characterization of self-phase modulation in liquid filled hollow core photonic bandgap fibers," J. Opt. Soc. Am. B **27**, 1886–1893 (2010).
10. A. R. Chraplyvy and T. J. Bridges, "Infrared generation by means of multiple-order stimulated Raman scattering in CCl_4- and $CBrCl_3$-filled hollow silica fibers," Opt. Lett. **6**(12), 632–633 (1981).
11. T. J. Bridges, A. R. Chraplyvy, J. G. Bergman, Jr., and R. M. Hart, "Broadband infrared generation in liquid-bromine-core optical fibers," Opt. Lett. **7**(11), 566–568 (1982).
12. G. S. He, J. D. Bhawalkar, C. F. Zhao, C. K. Park, and P. N. Prasad, "Two-photon-pumped cavity lasing in a dye-solution-filled hollow-fiber system," Opt. Lett. **20**(23), 2393–2395 (1995).
13. P. K. Dasgupta, Z. Genfa, S. K. Poruthoor, S. Caldwell, S. Dong, and S. Y. Liu, "High-sensitivity gas sensors based on gas-permeable liquid core waveguides and long-path absorbance detection," Anal. Chem. **70**(22), 4661–4669 (1998).
14. T. Dallas and P. K. Dasgupta, "Light at the end of the tunnel: recent analytical applications of liquid-core waveguides," TrAC-Trend, Anal. Chem. **23**, 385–392 (2004).
15. S. E. Harris and A. V. Sokolov, "Subfemtosecond pulse generation by molecular modulation," Phys. Rev. Lett. **81**(14), 2894–2897 (1998).
16. A. V. Sokolov, D. D. Yavuz, and S. E. Harris, "Subfemtosecond pulse generation by rotational molecular modulation," Opt. Lett. **24**(8), 557–559 (1999).

#161233 - $15.00 USD Received 11 Jan 2012; revised 20 Feb 2012; accepted 25 Feb 2012; published 23 Mar 2012

17. H. S. Rong, A. S. Liu, R. Jones, O. Cohen, D. Hak, R. Nicolaescu, A. Fang, and M. Paniccia, "An all-silicon Raman laser," Nature **433**(7023), 292–294 (2005).
18. F. Couny, F. Benabid, P. J. Roberts, P. S. Light, and M. G. Raymer, "Generation and photonic guidance of multi-octave optical-frequency combs," Science **318**(5853), 1118–1121 (2007).
19. A. M. Jones, A. V. V. Nampoothiri, A. Ratanavis, T. Fiedler, N. V. Wheeler, F. Couny, R. Kadel, F. Benabid, B. R. Washburn, K. L. Corwin, and W. Rudolph, "Mid-infrared gas filled photonic crystal fiber laser based on population inversion," Opt. Express **19**(3), 2309–2316 (2011).
20. N. Dudovich, D. Oron, and Y. Silberberg, "Single-pulse coherently controlled nonlinear Raman spectroscopy and microscopy," Nature **418**(6897), 512–514 (2002).
21. J. X. Cheng and X. S. Xie, "Coherent anti-Stokes Raman scattering microscopy: instrumentation, theory and applications," J. Phys. Chem. B **108**(3), 827–840 (2004).
22. C. W. Freudiger, W. Min, B. G. Saar, S. Lu, G. R. Holtom, C. W. He, J. C. Tsai, J. X. Kang, and X. S. Xie, "Label-free biomedical imaging with high sensitivity by stimulated Raman scattering microscopy," Science **322**(5909), 1857–1861 (2008).
23. G. P. Agrawal, *Nonlinear Fiber Optics* (Academic Press, San Diego, 2007).
24. M. J. Colles, "Efficient stimulated Raman scattering from picosecond pulses," Opt. Commun. **1**(4), 169–172 (1969).
25. N. Bloembergen and P. Lallemand, "Complex intensity-dependent index of refraction, frequency broadening of stimulated Raman lines, and stimulated Rayleigh scattering," Phys. Rev. Lett. **16**(3), 81–84 (1966).
26. A. Bertoni, "Analysis of the efficiency of a third order cascaded Raman operating at the wavelength of 1.24 μm," Opt. Quantum Electron. **29**(11), 1047–1058 (1997).
27. B. Min, T. J. Kippenberg, and K. J. Vahala, "Compact, fiber-compatible, cascaded Raman laser," Opt. Lett. **28**(17), 1507–1509 (2003).
28. A. D. Yablon, *Optical Fiber Fusion Splicing* (Heidelberg, Germany: Springer-Verlag press, 2005).
29. J. M. Hales, J. Matichak, S. Barlow, S. Ohira, K. Yesudas, J. L. Brédas, J. W. Perry, and S. R. Marder, "Design of polymethine dyes with large third-order optical nonlinearities and loss figures of merit," Science **327**(5972), 1485–1488 (2010).
30. M. J. Thorpe, K. D. Moll, R. J. Jones, B. Safdi, and J. Ye, "Broadband cavity ringdown spectroscopy for sensitive and rapid molecular detection," Science **311**(5767), 1595–1599 (2006).

1. Introduction

The liquid state of matter is widespread in nature and possesses outstanding optical properties. For that reason, researchers have been attempting to harness liquids (or fluids) for different applications in photonics [1, 2]. Liquid crystals are widely used for display. Besides that, it is quite difficult at the moment to find a real application in photonics that is based on this state of matter (dye lasers were widely used in the past but have become obsolete). The reason is the lack of suitable practical technology that allows working with long path-length liquids without the typical problems associated with diffraction, loss, and maintaining high intensity over the length. Liquid-core optical fiber (LCOF) was recognized very early [3, 4] as a great platform to investigate and explore optical properties of liquids. LCOF is normally created by filling a small capillary with an appropriate liquid which should be transparent at the wavelength of interest and have a refractive index slightly higher than that of the capillary's material to provide optical waveguiding via total internal reflection. Hollow-core photonics crystal fibers (HC-PCF) are also interesting structures where liquids or gases have been filled into the region around the hollow core. Several interesting applications of HC-PCF have been recently investigated [5–9]. These devices (LCOF and HC-PCF) make long interaction length with high optical field confinement possible, helping to enable nonlinear optical effects at extremely low power levels. Many interesting applications of LCOF have also been proposed and reported in the literature [10–14]. These prior works demonstrated the great potential of LCOF. However, early experiments required free space alignment to launch the light into the core of the LCOF rendering the use of liquid unpractical. Thus, even though promising results were obtained, the full potential of LCOF was not realized due to the lack of best performance and it has not been used in real applications. Here, we show that low loss fusion splicing of liquid core optical fiber to standard single-mode optical fiber not only results in an integrated practical and compact set-up but also it leads to about three-orders of magnitude better nonlinear performance compared with early experiments [5, 7]. As an example, we demonstrate ultra-low threshold of ~1 nJ stimulated Raman scattering in an integrated CS_2 filled LCOF pumped with sub-nanosecond pulses at 1064nm and 532nm compared with 800 nJ in prior experiments using hydrogen gas [5, 7].

#161233 - $15.00 USD Received 11 Jan 2012; revised 20 Feb 2012; accepted 25 Feb 2012; published 23 Mar 2012

2. Experiments and results

There are two suitable platforms that provide long interaction length and strong field confinement namely capillary tubing and HC-PCF. Generally, working with a liquid filled HC-PCF or capillary requires free space coupling into the small guiding core. It would be desirable to be able to splice these specialty fibers to standard singlemode fiber while still being able to fill the liquid of interest into the hollow region. To date, we have tried several different approaches to achieve this. Mechanical splicing is simple (there is always a small gap between the fibers for liquid access) but the structure is not very stable and the insertion loss is normally quite high. Femtosecond laser drilling after a regular splice is another interesting approach but creates small debris that could block the capillary creating significant power loss. The best approach that we have found so far is splicing standard single-mode fiber to the capillary while leaving a small gap for liquid access (see Fig. 1 below).

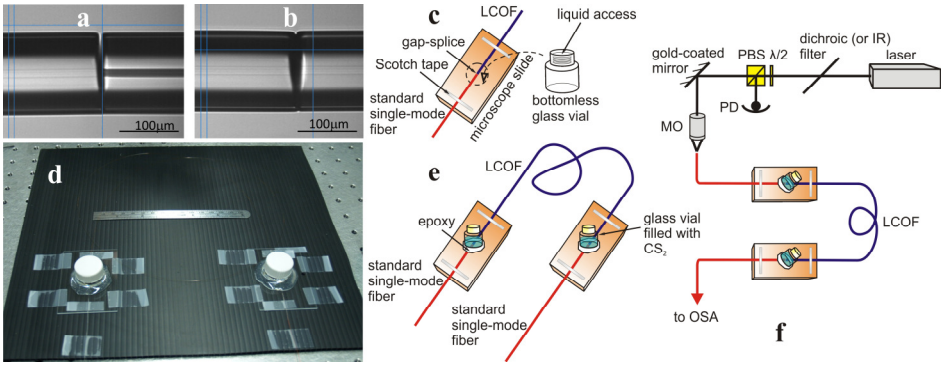

Fig. 1. Integrated LCOF preparation and stimulated Raman generation setup. **a**, Gap-splice between Corning SMF28 (left) and a 10µm core LCOF (right). **b**, Gap-splice between two segments of Corning SMF28. **c**, Liquid access port assembly. **d**, Photograph of an integrated 1m long LCOF filled with CS_2. **e**, Schematic of an integrated LCOF filled with CS_2. **f,** Schematic diagram of the experimental setup. PBS: polarizing beam splitter; MO: microscope objective; PD: photodiode; OSA: optical spectrum analyzer

In our experiments, we use fused silica capillaries. They have different inner tube diameters (10µm, 5µm and 2µm), the outer diameter is around 125µm matching well with standard single-mode fibers. To perform the splice, the capillary is cleaved at zero degrees (a straight angle) but the standard fiber is cleaved with an angle of 3-10 degrees (which helps to create a small gap after the fusion splice for liquid access). By optimizing the parameters of the heat source (Vytran FFS-2000 fusion splicer) hole-collapse could be avoided and a relatively strong joint with a small gap for liquid access could be formed (Fig. 1(a)). We have made a similar splice of SMF28 to another segment of SMF28 (Fig. 1(b)) and the loss of the transition was measured to be only around 0.1 dB. This indicates that the small gap left after the splice does not create appreciable loss. Due to the fact that the fibers are fused only in a small area the joint is not as strong as a standard fusion splice. However, the structure could be handled and transported (with some care) to a holder (access port) where it can be fixed permanently using an appropriate epoxy (Fig. 1(c)). A similar gap-splice is made at the other end of the capillary tubing at a certain length to create the second access port for liquid filling.

We use a mixture of CCl_4 and CS_2 (3-100% by volume depending on the size of the inner capillary) to fill the capillary of the LCOF. The choice of liquid is based on two following requirements: 1) the index of the liquid must be slightly higher than that of fused silica for guiding via total internal reflection while still maintaining single-mode operation; 2) the liquid should be transparent at the working wavelength (near-IR in our case). The filling was done by capillary action so no special equipment was needed. The refractive index (at around 1550nm) of CCl_4 is ~1.45 and that of CS_2 ~1.59. The concentration of CS_2 is varied to create the correct index contrast and numerical aperture of the guiding core to ensure single-mode operation. The optimal mixture of CCl_4 and CS_2 provides the ideal liquid refractive index,

#161233 - $15.00 USD Received 11 Jan 2012; revised 20 Feb 2012; accepted 25 Feb 2012; published 23 Mar 2012

making the LCOF single-mode so the transmission through the structure is very stable over time. Loss measurements were performed at around 1300 nm and 1550 nm for the LCOFs and the typical loss was ~15% for various chains of hybrid fibers (SMF28-LCOF (10μm diameter)-SMF28 or HI1060-LCOF (5μm diameter)-HI1060). The length of the LCOFs is around 1 m. For some of the chains we even observed as low as 5% total insertion loss. After filling with the liquid the access ports could be sealed and the structure remains stable for weeks (Figs. 1(d)-1(e)). This technique integrates LCOF with standard optical fiber in a compact and stable package without the need for free space alignment or complicated liquid handling procedures. It is surprising to note here that liquid filling of long fibers through the use of the capillary interaction works even with very small opening (down to 2μm in our case). What is the smallest size of the opening that it still works? We are doing research to answer this question since it may provide useful insights on the physics of capillary fluid dynamics. In addition, smaller core size also provides stronger field confinement which helps reduce the threshold of nonlinear processes further. To date, we have successfully used these devices in a few applications including Raman spectroscopy and switching, supercontinuum generation and low threshold Raman generation, as described below.

Stimulated Raman scattering (SRS) is a nonlinear optical process in which an incoming photon interacts with a coherently excited system resulting in generation of new frequencies with very high conversion efficiency. SRS is useful in wavelength conversion, amplification, generation of ultra-short (atto-second) optical pulses [15–19], precision spectroscopy and microscopy [20–22]. SRS occurs when the pump power reaches a certain threshold to provide enough gain for the Stokes wave. The threshold peak power can be estimated using the following simple formula [23]:

$$P^{thr} = 16\frac{A_{eff}}{g_R L_{eff}} \tag{1}$$

where in the present case the effective area is $Aeff = 3.14*10^{-12}$ m^2, the Raman gain coefficient for CS_2 is $g_R = 1.25*10^{-10}$ m/W at 532nm [24], and the effective interaction length is $L_{eff} = 1$m.

We used a frequency doubled microchip laser (JDSU) that emitted sub-nanosecond (~500ps) Q-switched pulses as the pump source. The repetition rate of the source was ~1.5kHz. The laser beam was coupled into a short piece (1m) of Corning HI1060 fiber using a microscope objective and translation stages, as shown in Fig. 1(f). The coupling efficiency was ~50%. The coupled power into the standard fiber was adjusted using a combination of a half waveplate and a polarizing beam splitter. For experiments in the visible, an IR filter was used to remove the residual 1064nm pulses. For experiments using 1064nm wavelength, the IR filter was replaced by a dichroic filter to remove the visible green beam. After the coupling step, light was launched into the integrated LCOF by simply splicing to the HI1060 fiber at one end. Figure 2(a) shows the evolution of the laser output after propagating through the CS_2 filled LCOF (The LCOF had a 2μm core diameter and was filled with 100% neat CS_2. Due to the mode mismatch between the LCOF and the standard coupling HI1060 fiber the total transmission of the device was ~30%). Several orders of Stokes Raman generation were seen as the pump power was increased. The threshold of stimulated Raman generation was at an extremely low pump pulse energy of ~1nJ. This energy threshold was near three orders of magnitude lower than the value reported for hydrogen filled HC-PCF of similar length [5]. The ultralow threshold observed in our experiment can be attributed to the unprecedented confinement of the optical field (~2μm core size), the long propagation length (~1m), and the large Raman gain coefficient of CS_2.

#161233 - $15.00 USD Received 11 Jan 2012; revised 20 Feb 2012; accepted 25 Feb 2012; published 23 Mar 2012

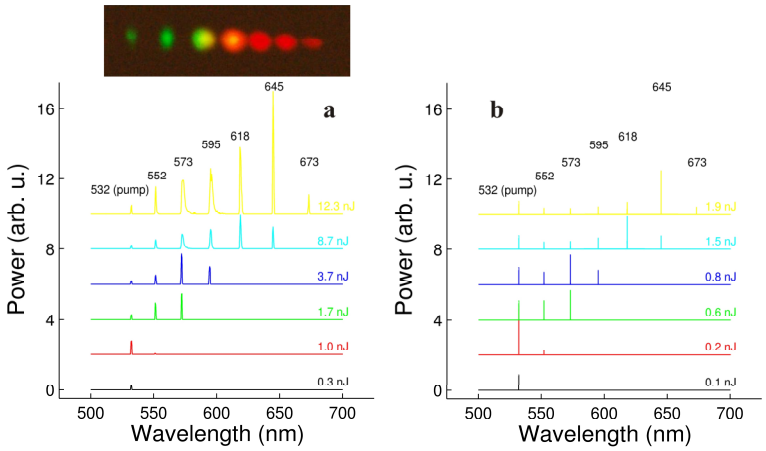

Fig. 2. Experimental and simulation results for 532nm pumping. Measured **a**) and calculated **b**) evolution of the output spectrum as the pump pulse energy is increased, for a pump wavelength of 532 nm. The numbers labeling the Stokes lines are the corresponding center wavelength in nanometers. Inset of **a**): Photograph of the Raman lines separated in space using a prism.

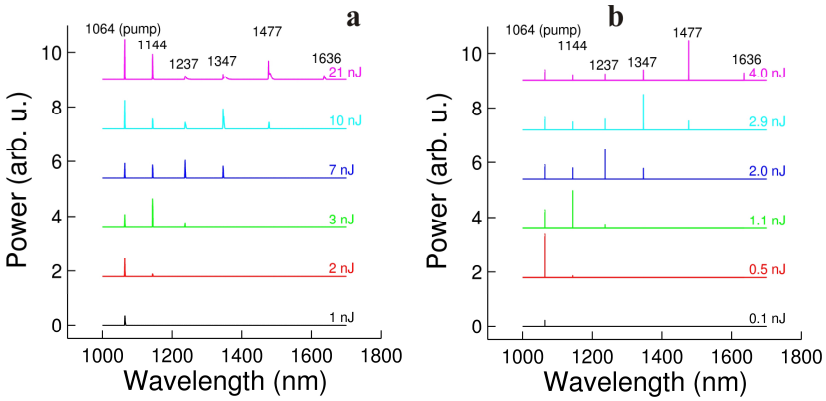

Fig. 3. Experimental and simulation results for 1064nm pumping. Measured **a**) and calculated **b**) evolution of the output spectrum as the pump pulse energy is increased for 1064nm pumping. Five orders of stimulated Raman scattering are generated at ~21nJ coupled pump pulse energy. The numbers labeling the Stokes lines are the corresponding center wavelength in nanometers.

Using Eq. (1), we obtain an estimated threshold pump peak power of 0.4W at 532 nm pump wavelength which is consistent with the low-power threshold observed experimentally (2W). We obtain the same threshold value when we numerically solve the coupled amplitude equations in the picosecond regime [23]. In Fig. 2(a), up to 6 orders of stimulated Raman scattering are generated at only ~12nJ of coupled pump pulse energy. We also observed broadening of the higher order Stokes lines. Broadening of stimulated Raman lines was also observed and explained by N. Bloembergen in Ref [25]. Detailed understanding of the difference in the level of broadening for different orders is quite complex and is beyond the scope of this paper. In the inset of Fig. 2(a), we nicely see multiple Raman lines that are separated in space using a prism made of SF10 glass. Due to the strong residual absorption of CS_2 at 532nm we observed gradual reduction in transmission of the pump light due to heating. The capillary was eventually (in matter of ~30 minutes) blocked and re-splicing of the fibers was required to observe the stimulated Raman generation process again. This thermally induced degradation was not observed when the fiber was pumped at 1064nm even at the highest available pulse energy (~300nJ) for a few weeks. We saw a similar trend when the laser wavelength was switched to 1064nm (Fig. 3(a)). The threshold of stimulated Raman

#161233 - $15.00 USD Received 11 Jan 2012; revised 20 Feb 2012; accepted 25 Feb 2012; published 23 Mar 2012

generation at this wavelength was also at an extremely low pump pulse energy of ~2nJ. Up to 5 orders of stimulated Raman scattering are generated at only ~21nJ of coupled pump pulse energy. We expect to see more Raman lines at higher pulse energies but they would be out of the measurement range of the OSA.

Calculations of the higher-order Stokes generation are carried out based on the coupled equations presented in Refs [26, 27]. Explicitly, these coupled equations read:

$$\frac{\partial A_p}{\partial z} = -\frac{g_p}{2}\left|A_{s,1}\right|^2 A_p \tag{2}$$

$$\frac{\partial A_{s,l}}{\partial z} = \frac{g_{s,l}}{2} | A_{s,l-1} |^2 A_{s,l} - \frac{g_{s,l}}{2}\left|A_{s,l+1}\right|^2 A_{s,l}, \quad l = 1,\ldots,M-1 \; (A_{s,0} \equiv A_p) \tag{3}$$

$$\frac{\partial A_{s,M}}{\partial z} = \frac{g_{s,M}}{2} | A_{s,M-1} |^2 A_{s,M} \tag{4}$$

The wavelength-dependent normalized (with respect to the effective area $g = g_R/A_{eff}$) Raman gain coefficients g_p and $g_{s,l}$ for the space-time dependent pump $A_p(z, t)$ and each Stokes line $A_{s,l}(z, t)$ up to the Mth order enter, respectively, while dispersion and nonlinearities have been neglected as a good approximation due to the long pump duration. Figure 2(b) shows the calculated output spectra for increasing pump pulse energies. We notice that the number and position of Raman lines and their relative heights are well reproduced by theory. We observe that up to 6 Raman orders are visible at a pump pulse energy of ~2 nJ. At lower pulse energies, only lower-order Raman lines are present, in good agreement with the experiment (Fig. 2(a)). The difference between experiment and theory can be explained by the variation of the core size along the fiber, uncertainties in the Raman gain coefficient and the partially polarized input pump (due to propagation through a long segment of non-polarization preserving fiber). Similar good match was also received when the laser wavelength was switched to 1064nm (Fig. 3(b))

The measured energy corresponding to the generation of different orders of stimulated Raman scattering is shown in Fig. 4(a). The threshold energy for the 1064 nm pump wavelength is higher than in the case of the 532nm pump, which is expected since the Raman gain coefficient is lower at longer wavelength [23, 28]. Figure 4(b) shows the corresponding calculations which are in good agreement with Fig. 4(a). We observe a linear dependence in the theory as observed in experiment for low pump powers (Fig. 4(a)). The deviation from the linear dependence as seen in the experimental data (Fig. 4(a)) at higher pump powers is conjectured to come from the higher absorption loss (due to water contamination) at longer wavelengths, or possibly reduced confinement and hence increased effective area for the longer wavelength Raman lines.

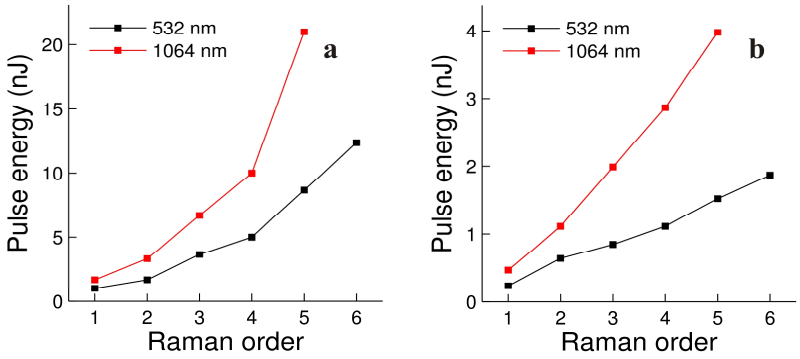

Fig. 4. Pulse energy threshold for generation of different Raman orders. The measured **a**) and calculated **b**) pulse energies corresponding to generation of different orders of Raman generation.

#161233 - $15.00 USD Received 11 Jan 2012; revised 20 Feb 2012; accepted 25 Feb 2012; published 23 Mar 2012

3. Conclusion

The reduction of Raman threshold power in LCOF should allow the use of low cost diode pumped lasers to create new frequencies. For example, we can envision the use of this platform to generate the required laser lines (red, green and blue) for future color TV display. Atto-second pulse generation via stimulated Raman scattering should also benefit from the low power threshold demonstrated here as well. The development of integrated LCOF is likely to lead to rapid progress of other important applications in nonlinear optics such as supercontinuum generation, mid-IR generation, slow light, all-optical switching and wavelength conversion. The prospects from practical liquid photonics appear to be quite bright. We further note that the recent development of organic materials [29] with tremendous molecular hyper-polarizability (~1000xCS_2) provides a route to pJ level operating energies. Research on designer molecules with ultrahigh Raman cross-section is an interesting area that has not been thoroughly investigated yet. There should be a lot of room for improvement that is awaiting to be fulfilled. In addition, the gap-splicing technique reported here can be used with HC-PCF to open up the possibility of using low index liquids or changing the gas under investigation on the same platform. This should be useful in applications involving gas sensing or breath analysis [30].

Acknowledgments

This work was supported in parts by the DARPA ZOE program (Grant No. W31P4Q-09-1-0012), the CIAN ERC (Grant No. EEC-0812072), and the USAF, AFRL COMAS MURI program (Grant No. FA9550-10-1-0558).

#161233 - $15.00 USD Received 11 Jan 2012; revised 20 Feb 2012; accepted 25 Feb 2012; published 23 Mar 2012